Journal of the Serbian Chemical Society
JSCS@tmf.bg.ac.rs • www.shd.org.rs/JSCS
J. Serb. Chem. Soc. 89 (10) 1387–1399 (2024)
JSCS–5794
Original scientific paper
Published 7 November, 2024

Joint characteristics and process parameters optimization on friction stir welding of AA 2024-T6 and AA 5083-H111 aluminum alloys

SAKTHIVEL SUNDARAM*• and MOHAN KUMARASAMY

Department of Mechanical Engineering, K.S. Rangasamy College of Technology, Tiruchengode-637215, Namakkal, Tamil Nadu, India

(Received 21 September, revised 21 November, accepted 22 December 2023)

Abstract: Friction stir welding (FSW) is a recent method for welding in a solid--state environments. The FSW parameters, namely pin rotation speed, welding speed, axial force and tool tilt angle affect weld joint microstructure and tensile strength. The study optimizes process settings to enhance mechanical properties and uses Response surface methodology (RSM) to predict the ultimate tensile strength (*UTS*) of FS-welded AA 2024-T6 and AA 5083-H111.These parameters must be understood in order to get optimal mechanical qualities in manufacturing. The created model predicted tensile strength within 5 % of experimental data, helping optimize process parameters for FSW joints. Tool tilt angle affects heat, material flow, defect generation, welding force, and friction stir weld joint quality.

Keywords: aluminum alloys; friction stir welding; optimization; tensile strength.

INTRODUCTION

A new approach for joining the metals in solid-state conditions is friction stir welding (FSW). This welding is called green welding since it does not emit oxide fumes as the conventional joining procedures do. A rotating pin is inserted into the material and moved along the joint line after “dwell time”. A weld junction forms as material flows from the advancing to the receding weldment. The friction between the tool and workpiece minimizes the flow stress around the pin and shoulder. In order to identify the complex flow pattern in a cylindrical tool, a friction stir forming model was developed by employing the particle streamline tracing techniques.[1] Dissimilar joints of AA 5083 and mild steel were evaluated.[2] The experimental design predicted the mechanical characteristics and microstructure

* Corresponding author. E-mail: sundaramsakthivel791@gmail.com
• S. Sakthivel is research Scholar at Dept. of Mech. Eng., K. S. Rangasamy College of Technology, Tiruchengode-637215, Namakkal, Tamil Nadu, India.
https://doi.org/10.2298/JSC230920100S

of the heterogeneous AA 5083-AA 6061 joints.[3] The results revealed that the tool rotation speed affected joint tensile characteristics more than tool pin diameter. FSW testing on AA 6351 and AA 5083 alloys used continuous plunging force, tool rotating speed, and welding speeds with different tool probes.[4] The data showed that straight square probe joints had higher tensile strength. The mechanical properties of dissimilar alloys of aluminum and copper at different tilt angles were examined, and a tool tilt angle of 4° produced defect-free joints with excellent strength and hardness.[5] FSW joints manufactured from 2024 and 7075 aluminum alloys showed a refined microstructure and good mechanical properties, including high tensile strength and flexibility. The effects of different circumstances on microstructure and mechanical qualities were studied using the optimal welding parameters for high-quality joints.[6] Al-2024 and Al-7039 weld joints with a heterogeneous composition of base metals were studied and the failure occurred when the Cu and Zn were in excess.[7] Dissimilar weld joints on AA 6061 and AA5052 alloys exhibited a fine-grained nugget zone with an equiaxed orientation.[8] RSM was used to create the regression models and examine the friction stir welding response variables. A mathematical model predicted the friction stir-welded 6061 aluminum alloy joint tensile strength.[9] The ultimate tensile strength, yield strength, and elongation of friction stir welded aluminum 5083-H111 and 6082-T6 alloys were examined.[10] FSW was done on AA 2024 and AA 6061 plates utilizing RSM to maximize elongation and ultimate strength with a suitable FSW pin profile.[11] The aluminum alloys of AA 6101-T6 and AA 1350 AA 5052 and AA 6101 plates were linked, and statistical analysis showed that traverse speed affected weld characteristics.[12,13] Rotational speed, welding speed, tool tilt angle, and axial force must be changed to produce these properties.[14] According to the literature, the researchers prefer RSM by employing different pin profiles for different materials to produce high-quality welds for aviation structural parts. To the authors' knowledge, AA 5083-H111 and AA 2024-T6 dissimilar joints are limited by the huge ranges of four parameters within the authorized scale. In this work, the authors focused on developing a statistical model to predict the strength of the joints within the selected range of parameters. The effects of the input parameters with respect to the tensile strength model will shed new light on the material science and engineering by the optimization of process parameters and characterizing FS welded AA 2024-T6 and AA 5083-H111 alloys.

EXPERIMENTAL PROCEDURE

Materials, methods, and experimentation

The study used 5 mm thick rolled AA 2024-T6 and AA 5083-H111 aluminum alloy plates cut to 100 mm×150 mm. Fig. 1a and b illustrate the clamping mechanism and weld joint sample used to hold the plates rigidly clamped in the fixture, respectively. The shank portion of the tool was held in the spindle. AA2024-T6 was fixed in the advancing side and in the retreating side AA5083- H111 was fixed. The rotating tool pin would plunge into the workpiece surface with

a dwell time, the required spindle speed, axial load, welding speed and tilt angles, which were given as input parameters to complete the weld. Owing to its increased stirring action and the material flow, high-carbon steel and non-consumable hexagon pin tools were used to fabricate the joints. The four-sided tool pin rotated well with the shear and mixed materials. The base metals in AA 2024-T6 are 93.35 Al, 4.3 Cu, 1.315 Mg, 0.522 Mn, 0.09 Si, 0.116 Fe, 0.041 Zn, 0.005 Cr, 0.005 Ni, 0.013 Ti and, for in AA5083, the constituent metals are 93.68 Al, 0.067 Cu, 4.8 Mg, 0.744 Mn, 0.1 Si, 0.231 Fe, 0.096 Zn, 0.092 Cr, 0.009 Ni, 0.017 Ti. Fig. 1c shows the specimen preparation of tensile strength as per ASTM E8 standard using electrical discharge machine. The base final tensile strengths of 397 and 316 MPa were achieved after the tensile test. The process parameters were varied by three levels and four parameters having the rotational speed of 600, 1050 and 1500 rpm, the traverse speed of 30, 45 and 60m/min and the tilt angle of 1, 2, 4 and 5°, and axial load of 3, 6 and 9 kN were chosen. The weld joints were subjected to the tensile testing machine having a load range of 5 tons with a load accuracy of 0.1 N and cross head speed accuracy of 0.01 mm. Initially, the samples are prepared for 10 mm×10 mm and it is mounted in the press and grinding is done using different grades of emery fineness papers, while polishing is carried out to remove scratches through a rotatable disc polishing machine, for microstructure analysis Weck's reagent is used (4 g $KMnO_4$, 1 g of NaOH and 100 mL H_2O for 20 s). Then the samples were subjected to close examination through the metallurgical microscope 5 MP camera and images were taken using De-winter Material plus version-2, Model JEOL JSM7001F for characterizing the weld joints by the scanning electron microscopy.

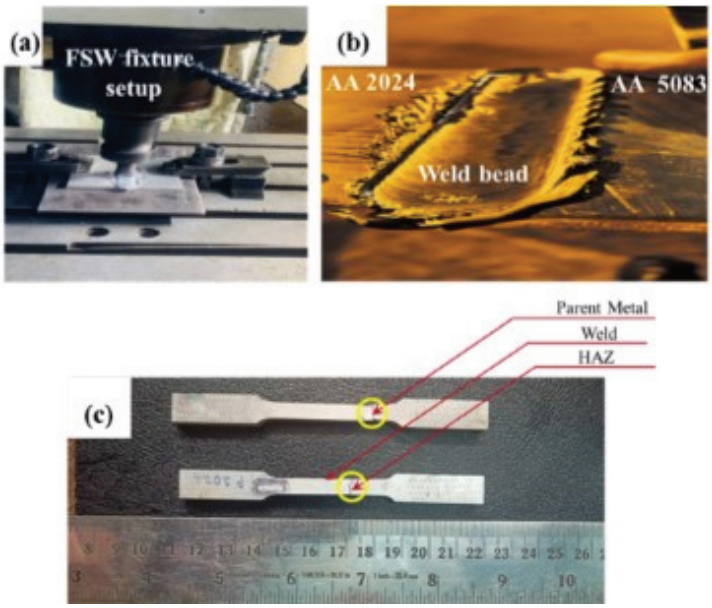

Fig. 1. a) Friction stir joining processes; b) FSW plate; c) fractured specimens.

RESULTS AND DISCUSSION

Welded joints with varied parameters were subjected to tests relating to tensile strength, and their results are discussed based on RSM; the microstructure and

fractography characterization are also discussed. Maximum and minimum tensile strengths of 320 and 284 MPa were obtained, as shown in Fig. 2.

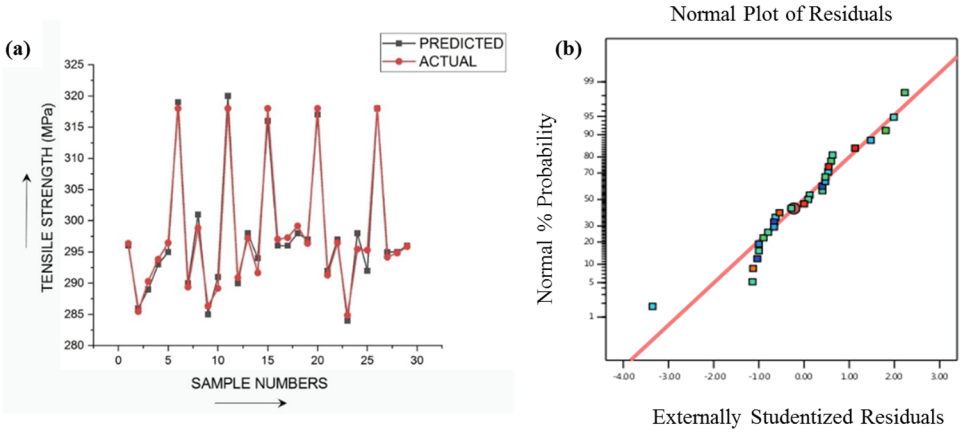

Fig. 2. a) Predicted *vs*. actual tensile strength; b) probability curve for predicted *vs*. actual tensile strength.

The TS response ANOVA results for the second-order polynomial regression model are presented in Table I. *F*-value and *P*-value determined the model and the coefficient significance. The model and coefficients were more significant, with a higher *F*-value and lower *P*-value. With an *F*-value of 8.3 and a *P*-value of 0.0001, the hypothesis is quite significant. If the *P*-value of the predicted coefficients is less than 0.05, the variables in the model are essential. If it was greater than 0.1, it was not significant. This model includes the major effects of welding speed (*B*), tilt angle (*C*) and axial load (*D*), the interaction terms *AB*, *AC* and *BC*; and the quadratic terms A^2, B^2, C^2 and D^2. According to the *F*-values, $D^2 > C^2 > B^2 > A^2 > BC > AC > AB > D > C > B$ were the most relevant parameters. The model is adequate with the estimated R^2 and adjusted R^2 values of 0.9809 and 0.9619, respectively. The multiple regression analysis of the experimental data yielded the following mathematical model in terms of coded parameters:

$$\text{Tensile strength} = 318.00 - 1.00A + 1.42B + 1.25C - 1.33D + 4.50AB + \\ + 4.50AC - 1.50AD - 5.00BC + 1.75BD + 0.7500CD - 14.00\,A^2 - \\ - 11.62\,B^2 - 12.38\,C^2 - 11.00\,D^2$$

Effect of tool rotational speed and welding speed

Choosing the correct tool rotational speed is essential for the welding success. It directly affects process heat generation, material flow and mixing.[15] Low rotating speed may not generate enough heat, resulting in poor material mixing and weak joints. Conversely, high rotational speeds can generate excessive heat, producing material flaws or tool wear.[16] A frequent case shows that tool rotation speed

impacts joint tensile strength, as seen in Fig. 3a and b. Joint tensile strength is lower than basic aluminum alloys at all tool rotating speeds. UTS escalates from 600 to 1050 rpm, and it lowers when the tool rotational speed is increased further.

TABLE I. ANOVA for tensile strength

Source	Sum of squares	*df*	Mean square	*F*-value	*P*-value	Model
Model	2885.71	14	206.12	51.45	< 0.0001	Significant
A-rotational speed	12	1	12	3	0.1055	
B-traverse speed	24.08	1	24.08	6.01	0.0279	
C-tilt angle	18.75	1	18.75	4.68	0.0483	
D-axial load	21.33	1	21.33	5.33	0.0368	
AB	81	1	81	20.22	0.0005	
AC	81	1	81	20.22	0.0005	
AD	9	1	9	2.25	0.1561	
BC	100	1	100	24.96	0.0002	
BD	12.25	1	12.25	3.06	0.1022	
CD	2.25	1	2.25	0.5617	0.466	
A^2	1271.35	1	1271.35	317.37	< 0.0001	
B^2	876.59	1	876.59	218.82	< 0.0001	
C^2	993.34	1	993.34	247.97	< 0.0001	
D^2	784.86	1	784.86	195.92	< 0.0001	
Residual	56.08	14	4.01			
Lack of fit	46.08	10	4.61	1.84	0.2915	Not significant
Pure error	10	4	2.5			
Cor Total	2941.79	28				
					R^2	0.9809
					Adjusted R^2	0.9619

Micro-voids and micro-tunnels occur in the nugget owing to the limited heat release at slow rotation, resulting in undesirable mechanical properties (Fig. 3b). The rotational speed promotes plasticizing metal heat and turbulent motion.[17] The range of tool rotational rates that can generate strong joints is restricted, and the UTS is particularly sensitive to speeds exceeding 1050 rpm. During FSW, friction and plastic deformation generate heat. The material yield strength and slide rate determine the deformation heat. At 600 rpm, the combined effects of heating and strain rate produce an IMC layer that is thin at the joint interface and does not spread IMCs in the stirred zone (SZ). A higher rotating speed may generate heat and material swirling to produce a thick intermetallic layer at the interface, particularly on the top side of the joint where the tool comes in contact. The frictional heat generation is 33 % higher at 1050 than at 600 rpm, resulting in a thicker IMC layer along the joints, which may explain the low tensile strength at this speed, as shown in Fig. 3c and d.

The tool generates 11 % less heat at 1050 than at 600 rpm; therefore, less intense material stirring may not be sufficient to form IMC across the contact,

especially in the lower joint farthest from the tool shoulder. The low joint strength may come from the 600 rpm base bonding. The FSW heat has increased the weaker zone of the foundation material, toughening it. High heat generation has delayed cooling, allowing the strengthening phases to recoil and coarse grains in the nugget to soften. Changing the tool speed creates a fine and sound weld zone with better efficiency. Precipitate dissolution, defect formation, grain coarsening, and micro--gap coalescence have weakened owing to the insufficient rotational speed of the tool (Fig. 3d).

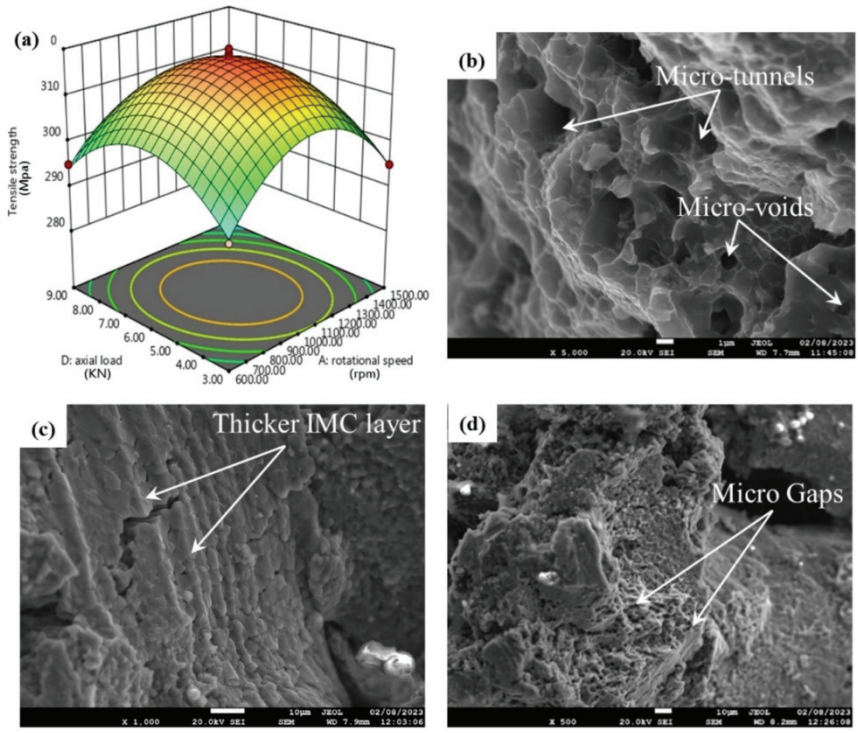

Fig. 3. a) Effect of tool rotational speed on tensile strength; b) micro-voids and micro-tunnels; c) thicker intermetallic layer (IMC); d) micro-gaps observed through scanning electron microscopy.

The tool moves along the joint at the welding speed. This severely affects the weld quality and integrity. The material flow, microstructural evolution, and heat input depend on the welding speed. The tool rotation speed, welding speed, tilt angle, axial force, and plunge depth affect the welded junction quality.[18] Fig. 4a shows the influence of welding speed in the tensile strength. The insufficient heat input at high welding speeds can result in incomplete mixing, top groove faults and material bonding.[19] Low welding speeds increase heat input, material distortion,

defects and metallurgical changes. Strong welds require the correct speed. Material mixing and bonding must be balanced by minimizing the heat input.

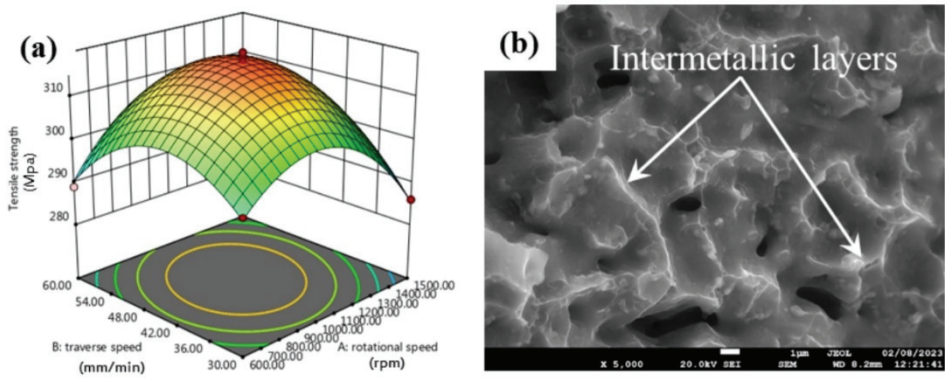

Fig. 4. a) The effect of welding speed on tensile strength; b) IMC layer at low welding speed.

The highest UTS is 45 mm/min. The UTS has changed proportionally with the welding speed on both sides of the maximum. The peak tensile strength of the joint has decreased by less than 10 %. Slow welding produces greater heat but less strain.[20] The speed of the welding has had a beneficial as well as detrimental impact on the formation of the interface IMC layer. Fig. 4b shows that when the welding speed has increased, the fewer IMCs are formed.[21] The heat has increased when the UTS declines from 30 to 45 mm/min. Moderate speeds provided a thin IMC layer at the interface, making the weld durable despite a high heat output. The UTS has dropped by 8 % with 60 mm/min welding. An increased FSW welding speed reduces metallurgical changes owing to the lower heat inputs and rapid joint cooling. Faster welding velocities provide less heat, but the IMC layer strain rate increases bond strength.[22]

Effect of axial load and tool tilt angle

Axial force is important in FSW, and it affects the weld strength and product quality. The axial force in FSW must be understood to obtain optimal results. The right axial force ensures a robust and consistent weld. This force helps to fuse materials together, resulting in a high-quality joint.[23] As shown in Fig. 5a, a low axial force might cause partial penetration and poor mixing of materials, reducing the weld strength.

The FSW joints have lost the tensile strength when the axial force is below 3 kN. The tensile strength has increased linearly from 3 to 6 kN. The tensile strength of the joint reduced when the axial force of 9 kN. All the welded joints exhibit this pattern, regardless of the tool inclination.

As can be seen in Fig. 6a the joints produced with AA 2024-T6 at a lower axial force of 3 kN have featured tunnel flaws on the advancing side of the joint,

leading to low tensile strength.[24] The weld joints subjected to a 9 kN axial stress have exhibited satisfactory welds; nevertheless, the presence of extra shear fractures on both sides have led to unfavorable tensile properties.

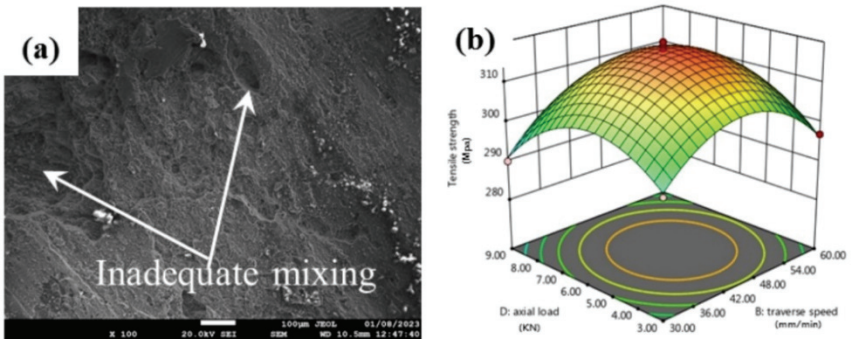

Fig. 5 a) Inadequate mixing observed through SEM; b) effect of welding speed on tensile strength.

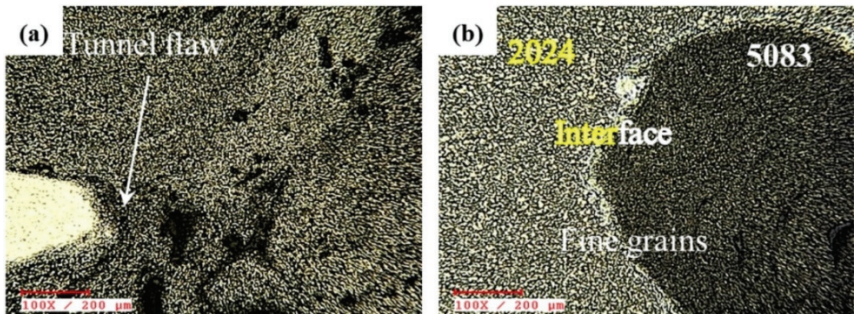

Fig. 6 a) Tunnel flaws defect in fabricated sample; b) material flow in the weld zone.

FSW frictionally heats, plasticizes, mixes, and extrudes two parts using a revolving pin-shoulder tool.[25] The linear weld load characteristics focus on the tool forces, particularly the shoulder force that governs the tool pin plunge depth into the workpiece. Tool rotation under static conditions can heat and plasticize the material. The shoulder force that controls the tool pin plunge depth into the workpiece changes significantly along the joint line. Extrusion moves the material after plastic deformation with applied forces and tool pin motion.[26] The extension of the tool pin into the workpiece depends on shoulder force.[27]

Fig. 7 shows the effect of the tool-tilt angle on the tensile strength. The inclination of the tool is relative to the workpiece surface.[28] The tool tilt angle affects the welding, the friction between the pins, and the plates are increase the heat with a larger tilt angle, which improves the material softening and mixing.[29] Void, porosity and weld joint penetration can result from an improper tool tilt angle.

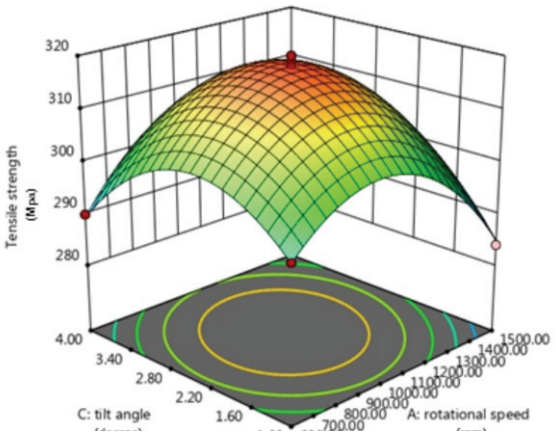

Fig. 7. Effect of tool tilt angle on tensile strength.

When the tool is tilted by 2.5°, the UTS drops by 1 % from the maximum value. The UTS decreases by 3 % when the tool tilt angle exceeds 4°. Tilting the tool enhances stirring, prevents shoulders from plunging, and increases the trailing side forging pressure, which consolidates the material.[30] However, tilting the tool beyond a certain degree affects the frictional coefficient, heat output, and material consolidation, causing the weld joint defects, including voids and pinholes, as shown in Fig. 8a. Thus, material mixing and coalescence under heat generation may explain the higher UTS projected at tool tilt angle of 2.5°. A review was conducted on the broad area of FSW and dealt with finding main process parameters of dissimilar alloys and prediction of mechanical behaviour of FSW joints. It is revealed that keeping tilt angles of 1 and 2.5° shows good plasticization besides avoiding the defects in the joints.[34]

Material straining and coalescence lower the UTS at lower tool tilt angles, heat production, and straining rate, and lower coalescence at tilt angles up to 2.5° as shown in Fig. 8b. The material strain rate increases when the tool tilt angle exceeds 4.5°; however, the effective drop in the heat output and material flow may induce a larger UTS drop. The movement of the elements and the mixing of the bonded materials improved as the tilt angle increased.[31] An improved material flow increased the mechanical characteristics of the weld joint. The mild UTS loss may be due to the reduced straining and coalescence at low tool tilt angles and increased straining rate, coalescence, and heat output at high tilt angles of up to 2.5°.

Characterization

The welding tool rotates and mixes the material, creating a unique onion ring structure, for maximum observed tensile strength of 320 MPa (Fig. 9a) which gradually transforms into a “V” shape pattern. Fig. 9b shows that the SZ formed a basin when the input heat has decreased or the cooling rate has increased. Without

the onion rings, the material viscosity improves, the strain rate increases, and the welding tool affects the material more.

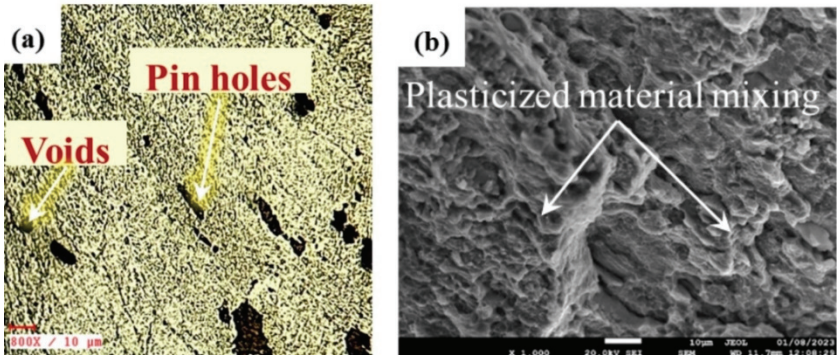

Fig. 8. a) Voids and pinholes; b) improved material mixing and coalescence during FS welding.

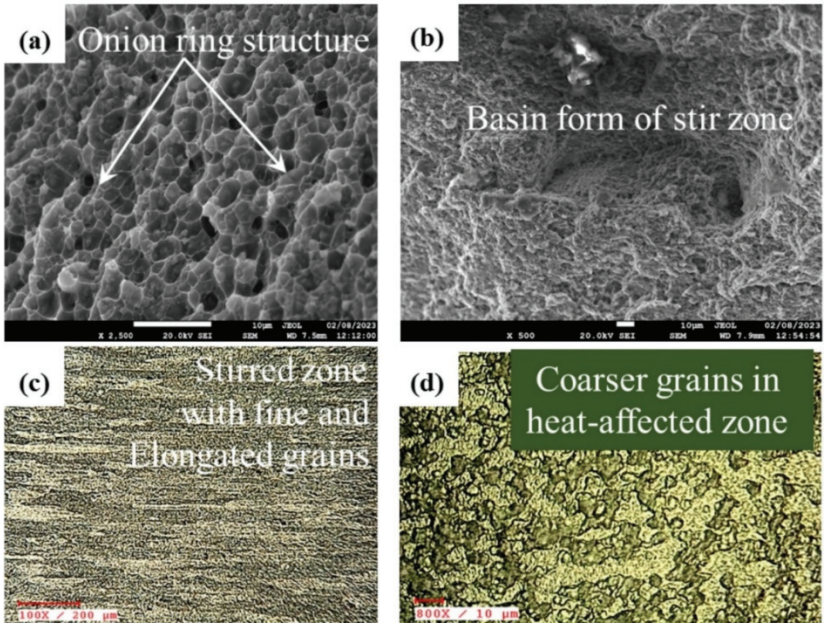

Fig. 9. a) Onion ring structure; b) basin form of stir zone; c) stirred zone (SZ); d) heat-affected zone (HAZ).

Fig. 9c illustrates the sample's stirred zone (SZ) and heat-affected zone (HAZ) cross-sectional microstructures. The dynamic recrystallization of aluminum grains is controlled by the temperature and cooling rate.[32,33] Many dislocations were observed in the induced grain boundaries when the magnification improved above 800×, as it is shown in Fig. 9d. Grain boundaries and recovery occur when there

are too many dislocations. During the mechanical stirring forced by the welding tool, these grain boundaries fluctuate and rotate. Recrystallized grains develop when the grain borders absorb the dislocations from the neighbouring grains.

CONCLUSIONS

- The friction stir welding was carried out using FSW machine and the maximum tensile strength was observed to be 320 MPa. From the ANOVA Table I it is concluded that the selected models are significant due to the value less than 0.0001.
- The R^2 value 0.9809 and the adjusted R^2 value 0.9619 are very close so that the predicted and the experimental values do not have much deviation.
- The increased heat generation and the material swirling at higher rotational rates may result in the creation of a thick IMC layer at the interface, particularly at the top portion of the joint where the tool shoulder engages.
- The inadequate bonding at the joint base at 600 rpm is likely to be the root because of its low joint strength.
- The forces produced by the tool, particularly the shoulder force that is directly responsible for the plunge depth of the tool pin into the workpiece, have been the primary focus of load characteristics associated with a linear weld.
- A greater decrease in the UTS is likely to have been caused by a decrease in heat production and material fusion when the tool tilt angle exceeds 4.5°, despite the increase in the substrate rate of strain.
- Varying the rate of welding has had both favorable and detrimental impacts on the IMC layer formation at the interface. By increasing the traverse speed, the degree of metallurgical changes may be reduced, the lower heat inputs are linked to the rapid cooling of the welded joint.

Acknowledgements. The authors are very much thankful to K. S. Rangasamy College of Technology.

ИЗВОД

КАРАКТЕРИСТИКЕ ЗАВАРЕНОГ СПОЈА И ОПТИМИЗАЦИЈА ПОСТУПКА ЗАВАРИВАЊА ТРЕЊЕМ МЕШАЊЕМ АЛУМИНИЈУМСКИХ ЛЕГУРА AA 2024-T6 И AA 5083-H111

SAKTHIVEL SUNDARAM и MOHAN KUMARASAMY

Department of Mechanical Engineering, K. S. Rangasamy College of Technology, Tiruchengode, Namakkal, Tamil Nadu, India

Заваривање трењем са мешањем (FSW) је савремени поступак спајања материјала у чврстом стању, без топљења и без употребе додатних супстанци. Најважнији параметри овог процеса: брзина ротације алата (трна), брзина заваривања, подужна сила и угао конуса алата (трна), утичу на карактеристике завареног споја, односно на микроструктуру и затезну чврстоћу. У овом раду је коришћена методологија одзивне површине (RSM) са циљем да се обезбеди могућност предвиђања и оптимизације затезне чврстоће завареног споја између легура AA 2024-T6 и AA 5083-H111. Разумевање утицаја свих параметара FSW поступка омогућава постизање оптималне чврстоће завареног споја. Вредности затезне чврстоће

добијене предвиђањем на основу модела, показале су добро слагање са експерименталним подацима, са одступањем у опсегу од 5 %. Показано је да угао конуса алата има велики утицај на генерисање топлоте, течење материјала, вредност силе, затим на појаву грешака, као и на квалитет завареног споја.

(Примљено 21. септембра, ревидирано 21. новембра, прихваћено 22. децембра 2023)

REFERENCES

1. T. Fagan, V. Lemiale, J. Nairn, Y. Ahuja, R. Ibrahim, Y. Estrin, *J. Mater. Process.* **231** (2016) 422 (https://doi.org/10.1016/j.jmatprotec.2016.01.009)
2. K. Kimapong, T. Watanabe, *Weld. J.* **83** (2004) 277
3. M. Ghaffarpour, M. Kazemi, M. J. Mohammadi Sefat, A. Azizand, K. Dehghani, *Proc. Inst. Mech. Eng., L* **231** (2017) 297 (https://doi.org/10.1177/1464420715595652)
4. R. Palanivel, P. K. Mathews, N. Murugan, I. Dinaharan, *Mater. Des.* **40** (2016) 7 (https://doi.org/10.1016/j.matdes.2012.03.027)
5. K.cP Mehta, V. J. Badheka, *Mater. Manuf. Process.* **31** (2016) 255 (https://doi.org/10.1080/10426914.2014.994754)
6. P. Cavaliere, E. Cerri, A. Squillace, *J. Mater. Sci.* **40** (2005) 3669 (https://doi.org/10.1007/s10853-005-0474-5)
7. C. Sharma, V. Upadhyay, B. S. Narwariya, *Mater. Res. Expres*s. **6** (2018) 026524 (https://doi.org/10.1088/2053-1591/aaeca3)
8. M. Sindhuja, S. Neelakrishnan, B. S. Davidson, *Mater. Res. Express.* **8** (2021) 106525 (https://doi.org/10.1088/2053-1591/ac2daf)
9. K. Elangovan, V. Balasubramanian, S. Babu, *Mater. Des.* **30** (2009) 188 (https://doi.org/10.1016/j.matdes.2008.04.037)
10. H. A. Kumar, V. V. Ramana, *Mater. Today: Proc.* **27** (2020) 951 (https://doi.org/10.1016/j.matpr.2020.01.270)
11. D. Vijayan, V. S. Rao, *Res. J. Appl. Sci. Eng.* **7** (2014) 4503 (http://dx.doi.org/10.19026/rjaset.7.827)
12. A. R. Kumar, R. Pandiyarajan, G. R. Raghav, K. J. Nagarajan, S. Rengarajan, S. D. Pandian, K. Sudhakar, *J. Chin. Inst. Eng.* **46** (2023) 81 (https://doi.org/10.1080/02533839.2022.2141338)
13. G. Kasirajan, S. Rengarajan, G. R. Raghav, V. S. Rao, K. J. Nagarajan, *Metall. Res. Technol.* **117** (2020) 405 (https://doi.org/10.1051/metal/2020039)
14. Z. Li, D. Lu, X. Gao, *J. Build. Eng.* **36** (2021) 102101 (http://doi.org/10.1016/j.jobe.2020.102101)
15. K. P. Mehta, V. J. Badheka, *Mater. Manuf. Process.* **31** (2016) 233 (https://doi.org/10.1080/10426914.2015.1025971)
16. P. Edwards, M. Ramulu, *Sci. Technol. Weld. Join.* **14** (2009) 669 (https://doi.org/10.1179/136217109X12464549883330)
17. S. S. Sabari, S. Malarvizhi, V. Balasubramanian, *J. Manuf. Process.* **22** (2016) 278 (https://doi.org/10.1016/j.jmapro.2016.03.014)
18. M. A. Wahid, A. N. Siddiquee, *Trans. Nonferrous Met. Soc.* **28** (2018) 193 (https://doi.org/10.1016/S1003-6326(18)64653-9)
19. P. Mastanaiah, A. Sharma, G. M. Reddy, *J. Mater. Process. Technol.* **257** (2018) 257 (https://doi.org/10.1016/j.jmatprotec.2018.03.002)
20. W. Xu, H. Wang, Y. Luo, W. Li, M. W. Fu, *J. Manuf. Process.* **35** (2018) 261 (https://doi.org/10.1016/j.jmapro.2018.07.028)

21. J. Verma, R. V. Taiwade, C. Reddy, R. K. Khatirkar, *Mater. Manuf. Process.* **33** (2018) 308 (https://doi.org/10.1080/10426914.2017.1291957)
22. Bagheri, M. Abbasi, F. Sharifi, A. Abdollahzadeh, *Met. Mater. Int.* **28** (2022) 2239 (https://doi.org/10.1007/s12540-021-01121-4)
23. V. P. Singh, S. K. Patel, N. Kumar, B. Kuriachen, *Sci. Technol. Weld. Join.* **24** (2019) 653 (https://doi.org/10.1080/13621718.2019.1567031)
24. M. Garg, A. Raturi, A. Bhattacharya, *Int. J. Adv. Manuf. Technol.* **105** (2019) 155 (https://doi.org/10.1007/s00170-019-04186-z)
25. R. K. Bhushan, D. Sharma, *Int. J. Mech. Mater. Eng.* **15** (2020) 1 (https://doi.org/10.1186/s40712-020-00119-x)
26. R. Kumar, V. Pancholi, *J. Manuf. Process.* **68** (2021) 1214 (https://doi.org/10.1016/j.jmapro.2021.06.051)
27. K. Elangovan, V. Balasubramanian, S. Babu, *J. Mater. Eng. Perform.* **17** (2008) 820 (https://doi.org/10.1007/s11665-008-9240-6)
28. M. Zhai, C. Wu, H. Su, *J. Manuf. Process.* **59** (2020) 98 (https://doi.org/10.1016/j.jmapro.2020.09.038)
29. X. Wang, Y. Xiao, L. Shi, M. Zhai, C. Wu, G. Chen, *J. Mater. Res. Technol.* **25** (2023) 38 (https://doi.org/10.1016/j.jmrt.2023.05.184)
30. D. Trimble, G. E. O'Donnell, J. Monaghan, *J. Manuf. Process.* **17** (2015) 141 (https://doi.org/10.1016/j.jmapro.2014.08.007)
31. N. Dialami, M. Cervera, M. Chiumenti, *Metals* **9** (2019) 1 (https://doi.org/10.3390/met9010028)
32. R. Saravanakumar, T. Rajasekaran, C. Pandey, *Proc. Inst. Mech. Eng., E* **237** (2022) 2334 (https://doi.org/10.1177/09544089221134446)
33. W. F. Xu, Y. X. Luo, M. W. Fu, *Mater. Charact*. **138** (2018) 48 (https://doi.org/10.1016/j.matchar.2018.01.051)
34. G. Di Bella, F. Favaloro, C. Borsellino, *Metals* **13** (2023) 1176 (https://doi.org/10.3390/met13071176).